IEEE Access
Multidisciplinary ⋮ Rapid Review ⋮ Open Access Journal

Received 23 September 2025, accepted 8 October 2025, date of publication 13 October 2025, date of current version 17 October 2025.

Digital Object Identifier 10.1109/ACCESS.2025.3620643

RESEARCH ARTICLE

Trade-Offs Between Fingerprinting and Self-Organizing Maps in RIS-Based Indoor Positioning

STANISLAVA SLAVOVA[1], NAVEED ALI KHAN[1,2], AND STEFAN SCHMID[1,2], (Member, IEEE)
[1]Internet Architecture and Management (INET), Technical University Berlin, 10623 Berlin, Germany
[2]Weizenbaum Institut, 10623 Berlin, Germany

Corresponding author: Naveed Ali Khan (naveed64@gmail.com)

The authors acknowledge the financial support by the Federal Ministry for Research, Technology and Space (BMFTR) in Germany in the programme of "Souverän. Digital. Vernetzt." Joint project 6G-RIC, project identification number: 16KISK0-PIN. Additionally, the authors acknowledge the financial support by the Federal Ministry of Education and Research of Germany (BMBF) under grant No. 16DII131 (Weizenbaum-Institut für die vernetzte Gesellschaft—Das Deutsche Internet-Institut).

ABSTRACT Indoor positioning is essential for applications such as smart manufacturing, logistics, healthcare, transportation, and immersive media. Conventional wireless methods can be unreliable indoors because obstacles like walls, interference, and reflections distort the signals and reduce accuracy. Reconfigurable Intelligent Surfaces (RIS) address these issues by reshaping wireless propagation. Programmable phase shifts create controlled diversity in the radio environment without extra infrastructure, improving the separability of fingerprints and enabling more reliable learning-based positioning. Fingerprinting with k-Nearest Neighbors (k-NN) remains a standard approach due to its simplicity, transparency, and low training cost. Self-Organizing Maps (SOM) provide an unsupervised alternative that captures hidden structures in the data and scales better with larger inputs but require dedicated training. A direct comparison of these two methods under RIS-assisted conditions clarifies how different algorithmic strategies respond to RIS-induced signal diversity. The evaluation uses real datasets collected under controlled RIS configurations. Both methods are tested under identical preprocessing and assessed for accuracy, computational efficiency, scalability, robustness to noise, and signal strength behavior. Results show that fingerprinting is more robust in small-scale or noisy environments with limited training resources, while SOM offers faster inference and more stable scaling with larger datasets. The benchmark identifies trade-offs that guide algorithm selection in RIS-assisted positioning for next-generation wireless systems.

INDEX TERMS Wireless localization, RIS, 6G, SOM, fingerprinting.

I. INTRODUCTION

Demand for indoor positioning has risen with wireless connectivity across many systems. Accurate location and tracking support smart environments, autonomous vehicles, emergency services, and AR. GPS and similar approaches under-perform indoors due to attenuation and multi-path, motivating research into alternative indoor methods. Reconfigurable Intelligent Surfaces (RIS) have been proposed as a solution to these challenges. By introducing programmable phase shifts, RIS reshape propagation, improve signal-to-noise ratio, extend coverage, and create controlled diversity in radio maps [1], [2], [3], [4], A single RIS can provide fingerprint separability without additional anchors, offering a cost-efficient way to improve accuracy [5]. Despite these advances, questions remain about how different machine learning techniques perform under RIS-assisted conditions. Fingerprinting with k-Nearest Neighbors (k-NN) is widely used due to its simplicity and low training cost, but it scales poorly with data size [6]. Self-Organizing Maps (SOM) represent an unsupervised alternative that organizes high-dimensional RSS data into topological grids, supporting faster inference and stable scaling after training [7], [8]. Comparing these two approaches under identical RIS datasets clarifies trade-offs in accuracy, efficiency, scalability, and robustness. Public RSS datasets with 20 and 90 RIS states enable such a benchmark while keeping the physical layout fixed [5]. The goal is method selection under practical

The associate editor coordinating the review of this manuscript and approving it for publication was Hang Shen.

constraints. Results indicate where fingerprinting is preferable for small databases and quick setup, and where SOM is preferable for low-latency inference at scale. RIS-induced diversity benefits both approaches by making features more discriminative [4], [5].

II. LITERATURE REVIEW

A. RIS FOR WIRELESS LOCALIZATION

RIS introduces element-wise phase control that reshapes propagation, improves SNR, and extends coverage, which supports positioning in cluttered interiors [4]. Recent experiments show adaptively programmable metasurfaces that react to scene changes and sustain performance in complex rooms [9]. Hardware with RF switch matrices validates low-cost panels and reveals practical constraints on phase resolution and update speed that influence localization cycles [10]. Multi-surface designs further improve geometric diversity and reduce the need for many active anchors, enabling positioning with fewer radio chains [11]. Deployment at scale raises system issues: configuration overhead grows with state count, channels drift over time, and energy budgets at the edge limit actuation and pilots, which calls for efficient control and monitoring strategies [12], [13], [14]. Survey work on RIS with edge computing summarises these trade-offs and highlights the need for repeatable datasets and benchmarks to compare algorithms fairly across identical states and layouts [1].

B. FINGERPRINTING FOR INDOOR LOCALIZATION

Fingerprinting estimates position by matching observed RSS to a radio map. It uses existing infrastructure and avoids geometric models, which simplifies deployment in buildings [6]. Accuracy depends on feature separability and map freshness. Device heterogeneity and layout changes degrade results. Normalisation, re-surveys, and interpolation mitigate drift and sparsity [15]. The k-NN family is the standard baseline. It is training-free but memory grows with database size and prediction time scales with the number of fingerprints. RIS helps by creating distinct radio maps under different states, which separates nearby positions without adding anchors [5]. The trade-off is control overhead and smart state selection.

C. MACHINE LEARNING IN RIS-AIDED LOCALIZATION

AI-driven surveys report strong interest in combining learning with RIS for fingerprinting, channel estimation, and beam control in 5G/6G systems [16], [17]. Deep models improve channel estimation under sparse pilots and structured priors, which stabilises downstream positioning [3], [18]. Neural optimisation can set transmit beams and RIS coefficients from second-order statistics, reducing reliance on instantaneous CSI that is hard to maintain indoors [19]. Heuristic-aided search narrows design spaces and lowers configuration cost for large panels [20]. Dimensionality reduction and clustering smooth radio map interpolation when sampling is sparse, improving generalisation across grids [15]. Graph neural networks extend joint optimisation to multi-RIS topologies, coordinating beamforming and reflections across panels [21]. At the same time, these methods raise deployment cost and data demands, and often depend on accurate CSI. Surveys on RIS with UAV relays and edge computing stress compute, energy, and reliability constraints that limit heavy models in embedded settings [12], [13]. A fair comparison therefore needs fixed datasets, identical preprocessing, and matched metrics to separate algorithm effects from data and control choices.

D. SELF-ORGANIZING MAPS IN WIRELESS NETWORKS

SOM offers unsupervised mapping from high-dimensional inputs to a two-dimensional grid while preserving local neighbourhoods, which supports clustering and anomaly detection in wireless data streams [7], [8]. The approach requires no labels during training and yields fast inference by best-matching unit lookup with centroid readout after training. These traits fit positioning tasks where labels are scarce or costly to refresh. In the RIS context, unsupervised mapping has been explored through MetaSLAM, which merges programmable propagation with SLAM-style learning to enhance localization without dense annotation [22]. MetaSLAM coordinates multiple RISs using a two-stage genetic and particle filter optimization to mitigate environmental variability, whereas our SOM-based approach adapts unsupervised mapping specifically for RIS state diversity, providing systematic benchmarks against strong fingerprinting baselines under identical RIS datasets. Public RSS datasets with multiple RIS states address reproducibility and enable controlled studies of accuracy, latency, memory, scalability, and noise tolerance under shared propagation conditions [5]. This gap motivates a side-by-side evaluation that reports when SOM or fingerprinting is the better choice and links outcomes to RIS-induced feature separability.

This paper has a structure as follows. The literature review can be found in Section II; the system model and the problem statement are given in Section III; the methodology is described in Section IV, and Section V introduces and discusses the experimental results.

III. SYSTEM MODEL AND PROBLEM STATEMENT

A. SYSTEM MODEL

We consider a RIS aided localization system that combines fingerprinting and SOM for accurate positioning in obstructed line-of-sight (LoS) environments. The system consists of the following key components:

* **Base Station (BS)**: Equipped with multiple antennas, responsible for transmitting signals.
* **Reconfigurable Intelligent Surface**: A passive array with N elements that dynamically modifies the wireless environment via phase shifts.
* **User Equipment (UE)**: A receiver located in an obstructed LOS environment, attempting to determine its location based on received signal characteristics.

The total channel between the BS and UE, considering the RIS, can be expressed as:

$$\mathbf{H}_{\text{total}} = \mathbf{H}_d + \mathbf{H}_r \Phi \mathbf{G} \tag{1}$$

where:

- $\mathbf{H}_d \in \mathbb{C}^{1\times M}$: The direct channel from the BS to the UE.
- $\mathbf{H}_r \in \mathbb{C}^{1\times N}$: The channel from the RIS to the UE.
- $\Phi = \text{diag}(e^{j\theta_1}, e^{j\theta_2}, \ldots, e^{j\theta_N})$: The diagonal matrix of RIS phase shifts.
- $\mathbf{G} \in \mathbb{C}^{N\times M}$: The channel matrix from the BS to the RIS.

The received signal at the UE is:

$$y = \mathbf{H}_{\text{total}} x + n \tag{2}$$

where:

- x : The transmitted pilot vector.
- $n \sim \mathcal{CN}(0, \sigma^2)$: Complex Gaussian noise with zero mean and variance σ^2.

1) RIS CONFIGURATIONS

The RIS has N elements, each with a tuneable impedance. Due to hardware limitations, the complex impedance values are quantized into D discrete levels. Therefore, the RIS can be in one of the following possible configurations:

$$|\mathcal{S}| = D^N \tag{3}$$

where:

- D: The number of quantization levels per element.
- N: The number of RIS elements.
- $|S|$: The number of distinct RIS configuration used to shape propagation data collection.

B. PROBLEM STATEMENT

Traditional fingerprinting based localization methods require multiple access points (APs) to ensure uniqueness. However, in a RIS assisted system, a single AP combined with an RIS can generate multiple distinct radio maps by adjusting RIS phase shifts.

1) FINGERPRINTING PROCESS

- **Offline Phase (Radio Map Creation)**:

$$\mathcal{R} = \{(\mathbf{r}_i, \mathbf{p}_i)\}_{i=1}^{|\mathcal{T}|} \tag{4}$$

where:

- $r_i \in R^d$: Fingerprint vector.
- $p_i \in R^2$ or R^3: Reference position.
- T: Number of fingerprints in the database.

- **Online Phase (Localization)**:

$$\hat{\mathbf{p}} = \arg\min_{\mathbf{p}_i \in \mathcal{R}} d(\mathbf{r}, \mathbf{r}_i) \tag{5}$$

where $d(\cdot,\cdot)$ is a distance metric.

We employed k Nearest Neighbors with distance based weighting:

$$\hat{p} = \frac{\sum_{i=1}^{k} w_i p_i}{\sum_{i=1}^{k} w_i}, \quad \text{where} \quad w_i = \frac{1}{\|r - r_i\|} \tag{6}$$

2) SOM BASED LOCALIZATION

Let $x = f(r)$. The $x = f(r)$ is preprocessed RSS vector. A SOM maps $x \in R^d$ to a 2D grid of neurons with weights w_j.

- **Best Matching Unit (BMU) selection:**

$$\hat{\mathbf{w}} = \arg\min_{\mathbf{w}_j} \|\mathbf{x} - \mathbf{w}_j\| \tag{7}$$

where:

- $\mathbf{w}_j$ represents the weight vectors of the SOM neurons.

- **Weight update:**

The weight update rule follows:

$$\mathbf{w}_j^{(t+1)} = \mathbf{w}_j^{(t)} + \eta(t) h_{j,b}(t)(\mathbf{x} - \mathbf{w}_j^{(t)}) \tag{8}$$

where:

- $\eta(t)$: The learning rate.
- $h_{j,b}(t)$: The neighborhood function centered at the BMU b.

After training, neuron weights $\mathbf{w}_j$ are associated with centroids of training labels $\mathbf{P}_j$. During inference, the predicted position is the centroid of $\mathbf{K}$ nearest neurons:

$$\hat{\mathbf{p}} = \sum_{j=1}^{K} \alpha_j \mathbf{p}_j \tag{9}$$

where:

- α_j are activation weights derived from neuron distances.

- **SOM adaptation to RIS dynamics:**

Inputs are RSS vectors over the active RIS state set (20 or 90). Features are normalized as follows: MinMax-normalized datasets for accuracy, efficiency, and noise experiments; additional z-score standardization for scalability. Training uses MiniSom with train random and linearly decaying learning rate $\eta(t)$ and neighborhood radius $\sigma(t)$. Euclidean distance is used for BMU selection. Grid size matches the experiment: 15×15 for accuracy, 25×25 for efficiency and noise, 30×30 for scalability, and 10×10 for signal-strength visualization. Iterations range from 2000 to 6000. Typical initial values are $\sigma_0 \in [0.8, 1.2]$ and $\eta_0 \in [0.3, 0.6]$. Each neuron stores the centroid of mapped training positions. Inference uses BMU-to-centroid readout (K=1). Equal, Random, and Uniform RIS configuration classes are included during training so the map remains stable under state permutations and statistical variation.

C. LOCALIZATION ERROR METRICS

- **Angular RMSE:** Measures deviation in predicted angles θ_t and true angles $\hat{\theta}_t$:

$$\text{RMSE} = \sqrt{\frac{1}{T}\sum_{t=1}^{T}(\theta_t - \hat{\theta}_t)^2}. \tag{10}$$

where:

- $\theta_t, \hat{\theta}_t$: True and estimated angles
- T: Number of evaluation samples

- **Linear Displacement:** Converts angular RMSE to meters using the arc length formula for a circular environment of radius r=5m

$$\text{Error}_m = r \cdot \frac{\pi}{180} \cdot \text{RMSE} \tag{11}$$

where:

- with $r = 5m$ as the fixed measurement radius used in the dataset [5].

D. DISTANCE METRIC SELECTION

The choice of distance metric D in BMU selection impacts localization performance:

- **Euclidean Distance:**

$$D(\mathbf{x}, \mathbf{y}) = \|\mathbf{x} - \mathbf{y}\| \tag{12}$$

where:

- $x, y \in \mathbb{R}^d$; x and y represent points in a d-dimensional real space ($\mathbb{R}^d$), and denotes the Euclidean norm, which computes the distance between the two points.

- **Structural Similarity Index (SSIM):**

$$\text{SSIM}(X, Y) = \frac{(2\mu_X\mu_Y + C_1)(2\sigma_{XY} + C_2)}{(\mu_X^2 + \mu_Y^2 + C_1)(\sigma_X^2 + \sigma_Y^2 + C_2)} \tag{13}$$

where:

- μ_X, μ_Y, σ_X^2, σ_Y^2, and σ_{XY} represent the mean and variance of X and Y. The constants are defined as $C_1 = (k_1 L)^2$ and $C_2 = (k_2 L)^2$, with window length L, $k_1 = 0.01$, and $k_2 = 0.03$. All main results use the Euclidean distance metric. SSIM is only applied in robustness ablations.

IV. METHODOLOGY

Evaluation follows a fixed pipeline: datasets and RIS states, preprocessing, algorithm settings, metrics, and experimental procedures. Figure 1 outlines the RIS-assisted setup with fingerprinting and SOM under identical conditions.

A. DATASETS

Two RSS datasets are used from the RIS fingerprinting setup of Nguyen et al. The files RIS_RXpower_dataset20 and RIS_RXpower_dataset90 record power at a grid of receiver positions under programmable RIS phase profiles. The first column encodes the RIS configuration. The remaining columns store RSS at several receiver orientations. The 20-state and 90-state sets induce different levels of signal diversity. Three configuration classes are present. Equal applies the same phase across elements. Random assigns phases without structure. Uniform follows a structured gradient. A separate beamforming file supports signal-strength visualization and links configuration IDs to phase vectors.

B. PREPROCESSING

Input vectors follow the project pipeline. Normalized CSVs are used directly for accuracy, efficiency, and noise experiments through MinMax scaling to [0,1]. Scalability applies z-score standardization on top of the normalized data using statistics from the training split and reuses the transform on the test split. Data are split 80/20 with seed 42. The same split feeds k-NN and SOM to ensure paired evaluation. No feature removal or imputation is applied. Outliers remain to reflect deployment noise.

C. ALGORITHMS

1) FINGERPRINTING (k-NN)

Matching uses Euclidean distance in RSS space. Predictions use inverse-distance weights wi=1r-ri over the k nearest references. Settings follow the scripts: k=4 for the 20-state set and k=20 for the 90-state set. Training stores fingerprints and coordinates. Inference performs brute-force search over the database used in training.

2) SELF-ORGANIZING MAPS (SOM)

Training uses MiniSom with random sampling. Learning rate and neighborhood radius decay linearly during training. Euclidean distance selects the best matching unit. Grids and hyperparameters mirror the code: 15×15, σ =0.8, learning rate 0.3, 2000 iterations for accuracy; 30×30, σ = 1.0, learning rate 0.5, 6000 iterations for scalability; 25×25, σ =1.2, learning rate 0.6, 5000 iterations for efficiency and noise; 10×10, σ = 1.2, learning rate 0.6, 5000 iterations for signal-strength visualization. Each neuron stores the centroid of mapped training positions. Inference reads out the BMU centroid, which corresponds to K=1. Training spans Equal, Random, and Uniform states so the map remains stable under state permutations and structured gradients. This adaptation aligns with prior SOM use in wireless data analysis and with unsupervised RIS-aided mapping.

D. METRICS

Localization accuracy follows angular RMSE as defined in Eq. (10). Conversion to meters uses Eq. (11) with r=5 m, consistent with the dataset geometry. Computational efficiency reports training time for k-NN storage and SOM training, and mean per-query prediction time over the test set. Scalability tracks latency and peak memory versus dataset size. Noise robustness measures RMSE under additive Gaussian noise injected at test time. Signal-strength behavior is analyzed with histograms and heatmaps across RIS states and with beamforming visualizations.

E. EXPERIMENTAL PROCEDURES

Accuracy uses one 80/20 split and reports mean and standard deviation over five runs with different shuffles of the training portion while the test portion remains fixed. Efficiency uses the same split. Timings rely on a high-resolution timer after a warm-up pass. Scalability evaluates subsample sizes of 500, 1000, 1500, and 1900 samples with five runs per size. Memory tracking uses tracemalloc and reports peak usage during training and prediction separately. Noise robustness injects Gaussian noise at 5, 10, 20, and 30 percent of each feature's

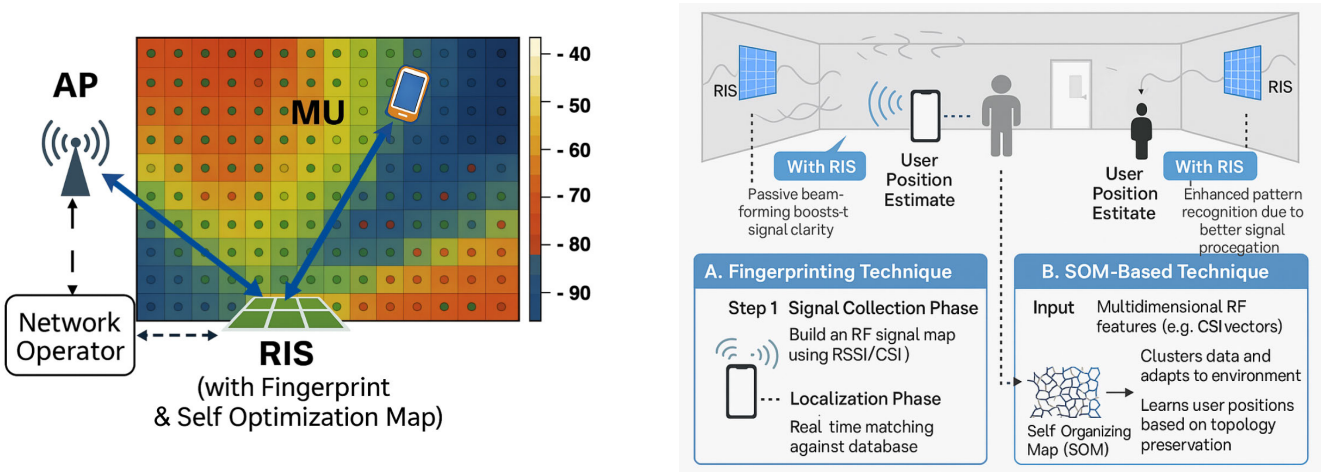

FIGURE 1. Fingerprint and SOM based wireless RIS-indoor localization framework with grid-based signal mapping.

standard deviation computed on the training split; training data remain unchanged. All ablations keep preprocessing, splits, seeds, and metrics identical across methods. SSIM appears only in robustness ablations; Euclidean distance supports all main results.

F. REPRODUCIBILITY

Environment uses Python 3.x with NumPy, scikit-learn, MiniSom, and Matplotlib. Seed 42 controls data splits and SOM initialization. Timings use time.perf_counter. Memory uses tracemalloc. Identical preprocessing, splits, and evaluation code paths are used for k-NN and SOM. Scripts reproduce all figures and tables.

V. RESULTS AND DISCUSSION

This section presents the evaluation of k-NN and SOM for RIS-assisted indoor localization. Results are structured along the five main axes: localization accuracy, computational efficiency, scalability, resilience to noise, and signal strength behavior under different RIS configurations. Beyond numerical outcomes, the section explains why the models perform as they do, how the RIS environment shapes their behavior, and what these findings mean for future deployments in 5G and 6G networks.

A. LOCALIZATION ACCURACY

Localization accuracy was measured using the Root Mean Square Error (RMSE) in angular degrees, which quantifies the difference between predicted and actual receiver positions on the circular grid of the dataset. Lower RMSE values indicate higher localization accuracy. For better interpretability, angular errors were also converted into linear distance errors using the known receiver–RIS separation of 5 meters. This conversion allows the results to be related to practical application requirements, such as navigation, XR, or industrial automation, where positional error in meters is the most meaningful metric.

Figure 2 shows the RMSE results for both k-NN and SOM on the two RIS datasets. In Dataset90, which contains 90 RIS states and therefore a rich variety of signal fingerprints, the two algorithms performed similarly. SOM achieved an angular RMSE of 43.19° (≈ 3.77 m), while k-NN reached 43.76° (≈ 3.82 m). The difference is small, but the edge for SOM indicates that its unsupervised mapping benefits from higher state diversity. With many RIS phase configurations producing distinct radio maps, SOM's neuron grid can capture the topology of the signal space more effectively. In this setting, the clustering power of SOM balances out its usual weakness in low-data regimes, and it even manages to slightly surpass k-NN.

On Dataset20, where only 20 RIS states are available, the story changes. k-NN achieved an angular RMSE of 33.01° (≈ 2.88 m), while SOM scored 44.16° (≈ 3.85 m). Here, k-NN's instance-based matching shows its advantage: with fewer states, fingerprints are more distinct, and direct comparison to stored references provides accurate predictions. SOM, on the other hand, struggles with limited diversity. Its unsupervised training compresses the input space into a fixed grid, and when the input variation is sparse, this representation becomes less precise. The result is an 11.15° accuracy gap in favor of k-NN.

The contrast between Dataset20 and Dataset90 highlights how dataset richness interacts with algorithm choice. k-NN is robust when data is limited and distinct, making it suitable for environments with few RIS configurations or constrained deployment scenarios. SOM gains ground when RIS diversity is high, where it can exploit structural learning to produce stable generalization. In practical terms, if a deployment can afford extensive RIS phase states, SOM may offer better accuracy; if RIS states are limited due to hardware or control restrictions, k-NN is the safer option.

It is also important to contextualize the accuracy values. Errors in the range of 2.8–3.8 meters are reasonable for RSS-based fingerprinting systems in indoor environments. While not sufficient for centimeter-level applications such as robotics in precision manufacturing, they are within acceptable bounds for user tracking, asset monitoring, or XR scenarios where sub-room-level positioning suffices.

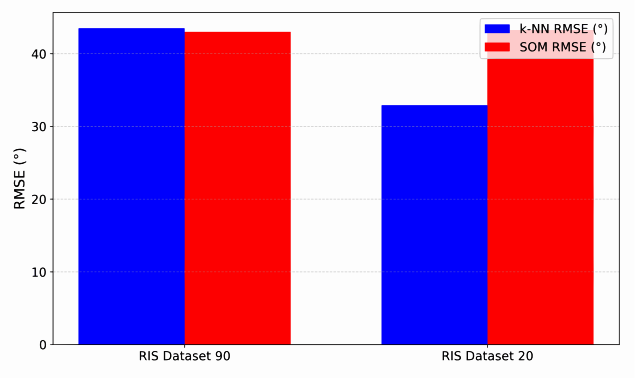

FIGURE 2. Localization accuracy (RMSE in degrees) of k-NN and SOM for RIS datasets with 90 and 20 beam configurations.

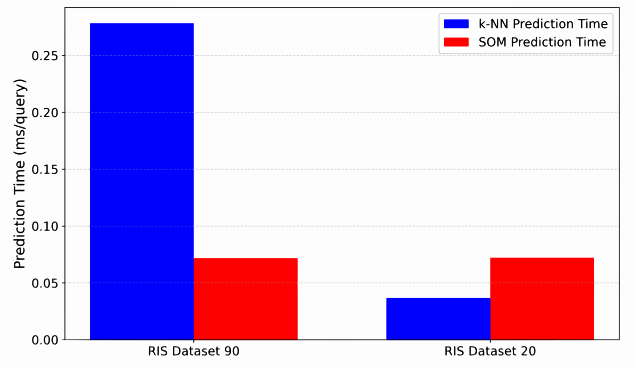

FIGURE 3. Training time comparison (log scale) between k-NN and SOM for RIS datasets.

Importantly, the results confirm that RIS phase diversity directly improves localization accuracy, as shown by the lower errors in Uniform configurations later discussed.

B. COMPUTATIONAL EFFICIENCY

Computational efficiency was evaluated in terms of training and prediction time. These metrics are critical in deciding whether a localization system can be deployed in real-time environments or on resource-constrained devices.

Training time k-NN has negligible training time because it does not construct an internal model; it simply stores the training samples. Across both datasets as shown in the Figure 3, training required less than 0.0005 seconds. SOM, in contrast, trains iteratively, updating neuron weights over thousands of iterations. Training required 0.582 seconds for Dataset90 and 0.584 seconds for Dataset20. This confirms the overhead associated with SOM: even when the dataset is smaller, the cost remains nearly constant because the training loop depends on fixed hyperparameters rather than dataset size.

Prediction time Prediction time is more relevant for real-time use, since it determines how quickly the system can estimate a new position. As shown in Figure 4, in Dataset90, k-NN required 0.41 ms per query, while SOM achieved 0.076 ms per query. On Dataset20, the difference was narrower: k-NN required 0.039 ms per

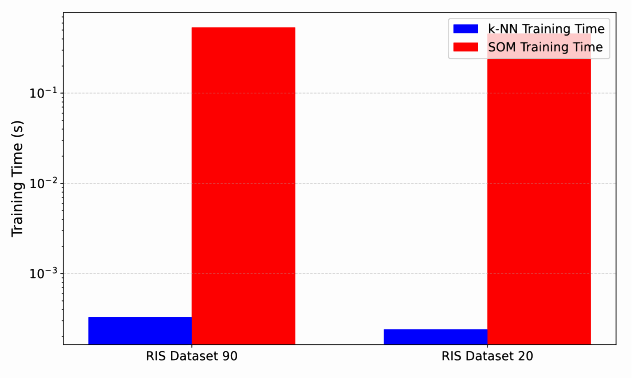

FIGURE 4. Prediction time (ms/query) comparison between k-NN and SOM across RIS datasets.

query, while SOM remained at 0.075 ms per query. These results reflect the fundamental trade-off: k-NN offers fast training but slower queries, while SOM requires longer training but provides faster inference. In deployments with frequent position updates (e.g., XR streaming or multi-user indoor navigation), SOM's stable inference speed offers an operational advantage. For systems that need instant setup with little training time (e.g., quick prototyping or emergency deployments), k-NN remains appealing.

It is also useful to compare these numbers to application demands. Sub-millisecond query times are well within the limits for most 5G and 6G applications, which typically tolerate latencies of tens of milliseconds. However, in scenarios with thousands of devices sending queries simultaneously, the difference between 0.41 ms and 0.07 ms per query can add up, making SOM more scalable in high-load environments.

C. SCALABILITY

Scalability analysis examined how accuracy, runtime, training time, and memory usage change as dataset size increases. Subsets of 500, 1000, 1500, and 1900 samples were used to simulate environments of different coverage densities.

1) EFFECT ON ACCURACY

As Figure 5 presents the RMSE trends in increasing dataset sizes. In Dataset90, SOM improved with dataset size. RMSE dropped from 64.1° at 500 samples to 45.15° at 1900. k-NN behaved in the opposite way, with RMSE rising from 22.52° to 43.93°. This is explained by the nature of instance-based matching. As more fingerprints are stored, neighboring samples become increasingly similar, making it harder for distance metrics to discriminate between them. SOM, however, benefits from denser training coverage, which allows its grid to map the RSS space more accurately. On Dataset20, a similar pattern appeared. SOM improved from 63.97° to 45.48°, while k-NN degraded from 11.66° to 33.69°. This confirms that k-NN excels with sparse training data, but SOM is more reliable as the dataset grows.

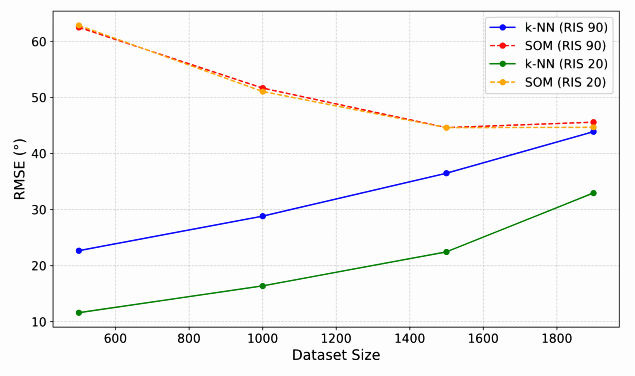

FIGURE 5. Scalability: RMSE vs. dataset size.

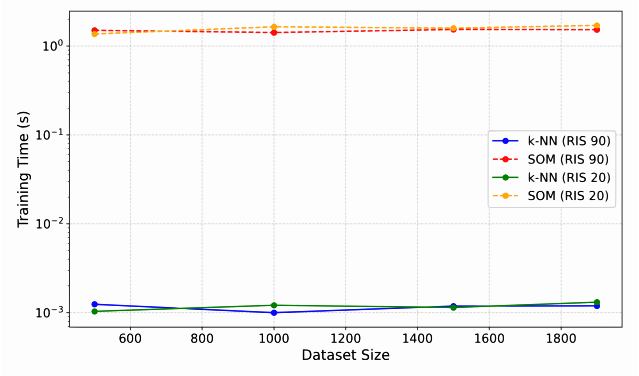

FIGURE 7. Scalability: training time vs. Dataset size.

2) EFFECT ON PREDICTION TIME

As Figure 6 illustrates prediction time per query. k-NN requires comparisons with every stored fingerprint. Prediction time is therefore sensitive to dataset size. On RIS 90, prediction time varied between 0.32 ms and 0.03 ms, with fluctuations due to cache effects. On RIS 20, the increase was steadier but still noticeable as size grew. SOM, by contrast, remained nearly constant at 0.055–0.063 ms/query, since it only searches its fixed grid of neurons. This stable inference time confirms SOM's scalability advantage.

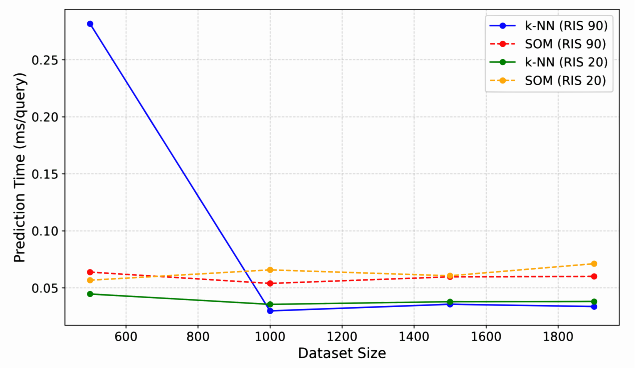

FIGURE 6. Scalability: prediction time vs. Dataset size.

3) EFFECT ON TRAINING TIME

k-NN training remained negligible at all sizes (<0.0012 s) as shown in the Figure 7. SOM training took 1.4 s across sizes, independent of dataset volume. This fixed overhead can be acceptable in static deployments where training is done once but is a limitation in dynamic environments where retraining is frequent.

4) EFFECT ON MEMORY USAGE

Figure 8 illustrates how memory usage changes with dataset size. SOM consistently used 985 kB because its memory cost depends on grid size, not dataset size. k-NN memory rose from 67 kB to 72 kB as more fingerprints were stored. In absolute terms, k-NN is lighter, but its memory grows linearly with dataset size, while SOM stays constant.

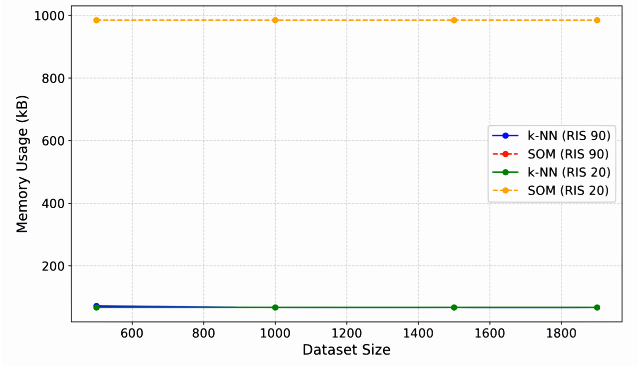

FIGURE 8. Scalability: memory usage vs. Dataset size.

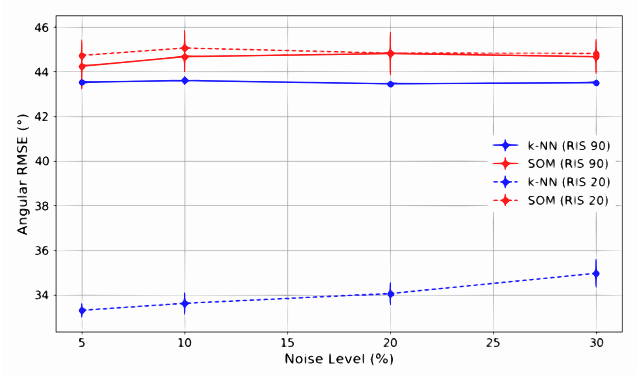

FIGURE 9. Robustness to noise: RMSE vs. noise level.

These trends illustrate the complementary strengths of the two approaches. k-NN is highly effective when training data is small and sparse, but it loses efficiency as the dataset grows. SOM scales better with larger datasets, delivering stable inference and improving accuracy with increased coverage. In practical terms, k-NN suits small-scale deployments such as a warehouse zone, while SOM fits larger deployments like a shopping mall or factory floor where dense fingerprints are available.

D. RESILIENCE TO NOISE

Real-world wireless environments suffer from interference, reflections, and hardware imperfections. To test robustness,

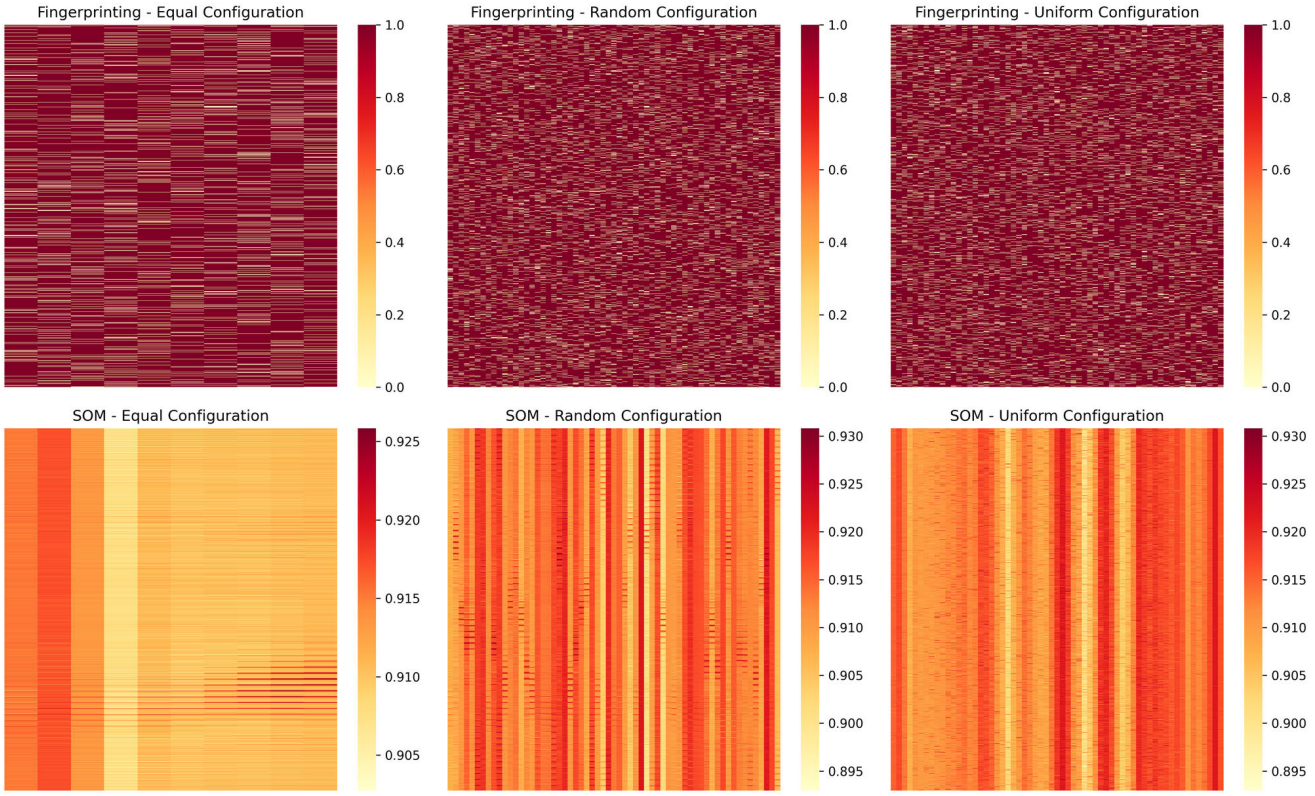

FIGURE 10. Signal strength comparisons.

TABLE 1. Comparative analysis of k-NN and SOM for localization metrics.

Metric	k-NN	SOM	Winner
Localization Accuracy (RMSE)	Lower on RIS 20	Lower on RIS 90	k-NN (avg.)
Training Time	$<$1 ms (all sizes)	$\approx$1.5 s (fixed)	k-NN
Prediction Time	0.03–0.32 ms/query	Stable at $\approx$0.06 ms	SOM
Memory Usage	70 kB (grows slightly)	$\approx$985 kB (fixed)	k-NN
Scalability (Accuracy)	Degrades with size	Improves with size	SOM
Noise Robustness	Stable across levels	Slight fluctuations	k-NN
Signal Strength Behavior	Good under structure	Learns under diversity	SOM

Gaussian noise at levels of 5%, 10%, 20%, and 30% was added to the test inputs. Training data remained unchanged.

Figure 9 shows the angular RMSE as a function of noise level. Whereas, in Dataset90, k-NN remained stable, with RMSE ranging 43.4°–43.6° even at 30% noise. SOM's RMSE ranged 44.1°–45.0°, showing small fluctuations but no dramatic degradation. On Dataset20, k-NN rose slightly from 33.3° to 35.1°, while SOM varied between 44.1° and 45.5°, indicating slightly higher sensitivity.

These results confirm that both models are reasonably robust to noise. k-NN's resilience comes from distance-weighted neighbor aggregation, which averages out noise across multiple references. SOM is somewhat more sensitive, since noise can distort the geometry of the RSS input space and cause neuron assignments to shift. However, the absolute differences remain small, and both models remain viable even under high noise levels. For practical deployments, this means that both models can tolerate interference typical of indoor networks, but k-NN may be safer in highly dynamic or uncontrolled environments.

E. SIGNAL STRENGTH BEHAVIOR AND RIS CONFIGURATIONS

The final analysis examined how RIS beamforming configurations influence localization. As illustrated in Figure 10, three configurations were tested: Equal, Random, and Uniform.

1) EQUAL CONFIGURATION

All RIS elements use identical phase shifts, producing a homogeneous signal field. Fingerprints lack diversity, making it difficult to distinguish locations. Both k-NN and SOM suffered higher errors. SOM's activation maps showed

weakly separated neuron clusters, and k-NN had difficulty retrieving unique nearest neighbors.

2) RANDOM CONFIGURATION

RIS elements apply random phases, increasing diversity but without structure. Heatmaps showed broad RSS distributions. SOM activated more neurons but in scattered, inconsistent clusters. k-NN gained from additional diversity but predictions were less stable across samples. Overall, results improved compared to Equal but were less reliable than Uniform.

3) UNIFORM CONFIGURATION

RIS elements were phase-shifted in a gradient, steering beams in structured directions. Heatmaps showed clear directional patterns. SOM formed compact, topologically consistent clusters. k-NN retrieved unique neighbors with higher confidence. Both methods achieved the lowest RMSE under Uniform, confirming that structured RIS configurations create discriminative fingerprints.

This analysis shows that RIS configuration design is as important as algorithm choice. Equal offers simplicity but poor separability. Random boosts diversity but lacks predictability. Uniform provides both diversity and spatial coherence, delivering the best accuracy. For deployment, this means RIS should be programmed with carefully chosen phase patterns rather than random settings.

F. DISCUSSION AND INSIGHTS

The results highlight clear trade-offs between k-NN and SOM in RIS-assisted localization:

- Accuracy: k-NN is better with limited states and sparse data; SOM benefits from high state diversity and dense fingerprints.
- Efficiency: k-NN enables instant setup but slower queries; SOM requires longer training but faster inference.
- Scalability: k-NN struggles as datasets grow; SOM improves with scale.
- Robustness: both are noise-tolerant; k-NN has a slight edge in unstable environments.
- RIS states: structured beamforming (Uniform) improves both methods and reduces error.

Table 1 presents a structured comparison highlighting which algorithm performed better under each metric.For system designers, the choice depends on deployment conditions. In small, static environments with limited RIS states, k-NN provides accuracy and simplicity. In large or dynamic deployments with high state diversity, SOM delivers scalability and low-latency inference. The broader implication is that RIS design and machine learning must be considered jointly. Algorithm performance depends not only on model structure but also on how RIS configurations create separable fingerprints. This integrated perspective supports the development of robust, RIS-aware localization systems for future wireless networks.

VI. CONCLUSION

This work presented a comparative evaluation of fingerprinting with k-NN and unsupervised learning with SOM in RIS-assisted indoor localization. Using two publicly available datasets with 20 and 90 RIS states, results were analyzed across localization accuracy, computational efficiency, scalability, robustness to noise, and signal strength behavior under different RIS configurations. The findings show that algorithm choice depends on RIS state diversity and system constraints. k-NN performed better when the number of RIS configurations was limited, offering strong accuracy and minimal training cost. However, it scales poorly as datasets grow, with rising prediction latency and reduced separability. SOM benefited from high state diversity, delivering stable inference, predictable memory usage, and improved accuracy with larger datasets. While training overhead is higher, SOM proved advantageous for real-time systems with frequent queries. Both methods tolerated noise well, though k-NN showed slightly stronger resilience in unstable conditions. Analysis of RIS configurations showed that structured phase profiles, particularly Uniform designs, improve fingerprint separability and lower error for both methods. Together, these insights demonstrate the importance of aligning algorithm selection with RIS programming. The results provide practical guidance for building scalable, robust, and efficient localization systems in 5G and 6G indoor environments.

REFERENCES

[1] M. Ahmed, S. Raza, A. A. Soofi, F. Khan, W. U. Khan, F. Xu, S. Chatzinotas, O. A. Dobre, and Z. Han, "A survey on reconfigurable intelligent surfaces assisted multi-access edge computing networks: State of the art and future challenges," *Comput. Sci. Rev.*, vol. 54, Nov. 2024, Art. no. 100668, doi: 10.1016/j.cosrev.2024.100668.

[2] Y. Zhao and J. He, "RISTA-reconfigurable intelligent surface technology," White Paper 282023, p. 29, 2023. [Online]. Available: http://www.risalliance.com/RISTA-Reconfigurable%20Intelligent%20Surface%20Technology% 20White%20Paper

[3] F. He, A. Harms, and L. Y. Yang, "Slow-moving channel estimation via Vandermonde structured tensor decomposition in RIS-aided MIMO systems," *IEEE Access*, vol. 12, pp. 67772–67783, 2024, doi: 10.1109/ACCESS.2024.3398427.

[4] Y. Liu, X. Liu, X. Mu, T. Hou, J. Xu, M. Di Renzo, and N. Al-Dhahir, "Reconfigurable intelligent surfaces: Principles and opportunities," *IEEE Commun. Surveys Tuts.*, vol. 23, no. 3, pp. 1546–1577, 3rd Quart., 2021, doi: 10.1109/COMST.2021.3077737.

[5] C. L. Nguyen, O. Georgiou, G. Gradoni, and M. Di Renzo, "Wireless fingerprinting localization in smart environments using reconfigurable intelligent surfaces," *IEEE Access*, vol. 9, pp. 135526–135541, 2021, doi: 10.1109/ACCESS.2021.3115596.

[6] Y. Yang, M. Chen, Y. Blankenship, J. Lee, Z. Ghassemlooy, J. Cheng, and S. Mao, "Positioning using wireless networks: Applications, recent progress, and future challenges," *IEEE J. Sel. Areas Commun.*, vol. 42, no. 9, pp. 2149–2178, Sep. 2024, doi: 10.1109/JSAC.2024.3423629.

[7] Y. Miftahuddin and A. R. S. Ridwan, "Application of self-organizing map and K-means to cluster bandwidth usage patterns in campus environment," *Jurnal Online Informatika*, vol. 10, no. 1, pp. 66–76, Apr. 2025, doi: 10.15575/join.v10i1.1438.

[8] A. Panwar and S. J. Nanda, "Data analysis in wireless sensor networks with distributed self organizing map," in *Proc. IEEE 1st Int. Conf. Adv. Signal Process., Power, Commun., Comput. (ASPCC)*, Dec. 2024, pp. 61–66, doi: 10.1109/ASPCC62191.2024.10881504.

[9] H. Q. Yang, J. Y. Dai, H. D. Li, L. Wu, Z. H. Shen, Q. Y. Zhou, M. Z. Zhang, S. R. Wang, Z. X. Wang, J. W. Wu, S. Jin, W. Tang, Q. Cheng, and T. J. Cui, "Adaptively programmable metasurface for intelligent wireless communications in complex environments," *Nature Commun.*, vol. 16, no. 1, Jul. 2025, Art. no. 6070, doi: 10.1038/s41467-025-61409-6.

[10] M. Rossanese, P. Mursia, A. Garcia-Saavedra, V. Sciancalepore, A. Asadi, and X. Costa-Perez, "Designing, building, and characterizing RF switch-based reconfigurable intelligent surfaces," in *Proc. 16th ACM Workshop Wireless Netw. Testbeds, Exp. Eval. CHaracterization*, Oct. 2022, pp. 69–76, doi: 10.1145/3556564.3558236.

[11] G. C. Alexandropoulos, I. Vinieratou, and H. Wymeersch, "Localization via multiple reconfigurable intelligent surfaces equipped with single receive RF chains," *IEEE Wireless Commun. Lett.*, vol. 11, no. 5, pp. 1072–1076, May 2022, doi: 10.1109/LWC.2022.3156427.

[12] M. Ahmed, A. A. Soofi, S. Raza, F. Khan, S. Ahmad, W. U. Khan, M. Asif, F. Xu, and Z. Han, "Advancements in RIS-assisted UAV for empowering multiaccess edge computing: A survey," *IEEE Internet Things J.*, vol. 12, no. 6, pp. 6325–6346, Mar. 2025, doi: 10.1109/JIOT.2025.3527041.

[13] E. Tohidi, M. Franke, C. V. Phung, N. Khan, A. Drummond, S. Schmid, A. Jukan, and S. Stańczak, "Reliability assurance in RIS-assisted 6G campus networks," in *Proc. 20th Int. Conf. Design Reliable Commun. Netw. (DRCN)*, May 2024, pp. 107–114, doi: 10.1109/DRCN60692.2024.10539144.

[14] S. Li, B. Duo, X. Yuan, Y.-C. Liang, and M. Di Renzo, "Reconfigurable intelligent surface assisted UAV communication: Joint trajectory design and passive beamforming," *IEEE Wireless Commun. Lett.*, vol. 9, no. 5, pp. 716–720, May 2020, doi: 10.1109/LWC.2020.2966705.

[15] H. W. Khoo, Y. H. Ng, and C. K. Tan, "Enhanced radio map interpolation methods based on dimensionality reduction and clustering," *Electronics*, vol. 11, no. 16, p. 2581, Aug. 2022, doi: 10.3390/electronics11162581.

[16] G. Pan, Y. Gao, Y. Gao, W. Yu, Z. Zhong, X. Yang, X. Guo, and S. Xu, "AI-driven wireless positioning: Fundamentals, standards, State-of-the-art, and challenges," 2025, *arXiv:2501.14970*.

[17] N. A. Khan and S. Schmid, "AI-RAN in 6G networks: State-of-the-art and challenges," *IEEE Open J. Commun. Soc.*, vol. 5, pp. 294–311, 2024, doi: 10.1109/OJCOMS.2023.3343069.

[18] T. C. Rapudu and O. O. Oyerinde, "Machine learning-based channel estimation for multi-RIS-assisted mmWave massive-MIMO OFDM system in a dynamic environment," *IEEE Trans. Wireless Commun.*, vol. 24, no. 6, pp. 5297–5309, Jun. 2025, doi: 10.1109/TWC.2025.3546671.

[19] K. T. Kyaw, W. Santipach, K. Mamat, K. Kaemarungsi, K. Fukawa, and L. Wuttisittikulkij, "Neural network based optimization of transmit beamforming and RIS coefficients using channel covariances in MISO downlink," *AEU - Int. J. Electron. Commun.*, vol. 191, Feb. 2025, Art. no. 155656, doi: 10.1016/j.aeue.2024.155656.

[20] H. Zhou, M. Erol-Kantarci, Y. Liu, and H. V. Poor, "Heuristic algorithms for RIS-assisted wireless networks: Exploring heuristic-aided machine learning," *IEEE Wireless Commun.*, vol. 31, no. 4, pp. 106–114, Aug. 2024, doi: 10.1109/MWC.010.2300321.

[21] B. Lim and M. Vu, "Graph neural network based beamforming and RIS reflection design in a multi-RIS assisted wireless network," 2025, *arXiv:2501.14987*.

[22] Z. Yang, H. Zhang, H. Zhang, B. Di, M. Dong, L. Yang, and L. Song, "MetaSLAM: Wireless simultaneous localization and mapping using reconfigurable intelligent surfaces," *IEEE Trans. Wireless Commun.*, vol. 22, no. 4, pp. 2606–2620, Apr. 2023, doi: 10.1109/TWC.2022.3213053.

STANISLAVA SLAVOVA is currently pursuing the B.Sc. degree in business informatics with Technische Universität Berlin, Germany. She works at KPMG in the field of information technology, where she contributes to projects involving data analysis, system optimization, and business applications support. Alongside her professional role, she has an interest in applying technology to solve practical problems, with a particular focus on wireless communication, smart environments, and data-driven decision making. Her skills include working with Python, data processing, and machine learning techniques. She aims to combine her academic background with industry experience to develop innovative solutions for modern digital infrastructures.

NAVEED ALI KHAN received the Bachelor of Science degree in electronics engineering from the Sir Syed University of Technology, Karachi, Pakistan, in 2003, the M.Sc. degree in computer and communication networks from TELECOM and Management SudParis (ex INT), Evry, France, in 2006, and the Ph.D. degree in communication and information systems from the School of Electronics Information and Electrical, Dalian University of Technology, China, in 2016. He is currently a Postdoctoral Scholar with 6G-RIC, Digital Economy and the Internet Ecosystem, TU-Berlin, and Weizenbaum Institute, Germany.

STEFAN SCHMID (Member, IEEE) received the M.Sc. and Ph.D. degrees from ETH Zurich. He completed postdoctoral research at TU Munich and the University of Paderborn. He is currently a Professor with the Technical University of Berlin, Germany, working part-time at the Fraunhofer Institute for Secure Information Technology (SIT), Germany, and at the Faculty of Computer Science, University of Vienna, Austria. He is a Senior Research Scientist with T-Labs, Berlin, an Associate Professor with Aalborg University, Denmark, and a Full Professor with the University of Vienna. He received the IEEE Communications Society ITC Early Career Award 2016 and an ERC Consolidator Grant 2019.